Vol 467|9 September 2010|doi:10.1038/nature09379

LETTERS

Graphene as a subnanometre trans-electrode membrane

S. Garaj[1], W. Hubbard[2], A. Reina[3], J. Kong[4], D. Branton[5] & J. A. Golovchenko[1,2]

Isolated, atomically thin conducting membranes of graphite, called graphene, have recently been the subject of intense research with the hope that practical applications in fields ranging from electronics to energy science will emerge[1]. The atomic thinness, stability and electrical sensitivity of graphene motivated us to investigate the potential use of graphene membranes and graphene nanopores to characterize single molecules of DNA in ionic solution. Here we show that when immersed in an ionic solution, a layer of graphene becomes a new electrochemical structure that we call a trans-electrode. The trans-electrode's unique properties are the consequence of the atomic-scale proximity of its two opposing liquid–solid interfaces together with graphene's well known in-plane conductivity. We show that several trans-electrode properties are revealed by ionic conductance measurements on a graphene membrane that separates two aqueous ionic solutions. Although our membranes are only one to two atomic layers[2,3] thick, we find they are remarkable ionic insulators with a very small stable conductance that depends on the ion species in solution. Electrical measurements on graphene membranes in which a single nanopore has been drilled show that the membrane's effective insulating thickness is less than one nanometre. This small effective thickness makes graphene an ideal substrate for very high resolution, high throughput nanopore-based single-molecule detectors. The sensitivity of graphene's in-plane electronic conductivity to its immediate surface environment and trans-membrane solution potentials will offer new insights into atomic surface processes and sensor development opportunities.

We measured the ionic conductance of a 0.5×0.5 mm, chemical vapour deposition (CVD)-grown[2,3], sheet of graphene mounted across the surface of a 200×200 nm aperture in a 250-nm-thick, free-standing, insulating SiN_x layer on a Si substrate chip (Fig. 1). The electronic properties are measured across the sheet electrode, from one face to the other, hence 'trans-electrode'. Spatially resolved micro-Raman spectra of the G, G′ peaks from the graphene showed it to consist of a mixture of one-layer and two-layer domains[3,4], with a domain size of ~10 μm. The chip-mounted membrane was inserted in a fluidic cell so that it separated two compartments, each subsequently filled with ionic solutions electrically contacted with Ag/AgCl electrodes. The small diameters of the polydimethylsiloxane (PDMS) seals in the fluidic cell precluded ionic solution from leaking around the edges of the graphene.

With 100 mV bias applied between the two Ag/AgCl electrodes, current measurements in a variety of chloride electrolytes show that the conductance across the graphene membrane is far below the nanosiemen level (Table 1). The highest conductances are observed for solutions with the largest cations, Cs and Rb, correlated with a minimal hydration shell that mediates their interaction with the graphene[5,6]. We attribute this conductance to ion transport through defect structures in the free-standing graphene. Contributions from electrochemical currents to and from the graphene can be ruled out (Methods). The observed conductances for different cations falls much faster than the solution conductivities on going from CsCl to LiCl (Table 1), suggesting an influence of graphene–cation interactions. Nevertheless, we cannot completely rule out ionic transport through graphene that is in contact with the chip surface. Small asymmetries and nonlinearities in the current–voltage (I–V) curves were observed in the data for Table 1 and elsewhere (for example, Fig. 2), reflecting asymmetrical properties of the graphene surfaces associated with its CVD growth[3] or transfer to the chip.

A single nanometre-scale pore[7] (produced by electron-beam drilling) in the graphene trans-electrode membrane increases its ionic conductance by orders of magnitude (Fig. 2). Experiments with known nanopore diameters and solution conductivities allow us to deduce graphene's effective insulating thickness. The ionic conductance G of a pore of diameter d in an infinitely thin insulating membrane is given by[8]

$$G = \sigma d \tag{1}$$

where $\sigma = F(\mu_K + \mu_{Cl})c$ is the conductivity of the ionic solution, F is the Faraday constant, c is ionic concentration, and $\mu_i(c)$ is the

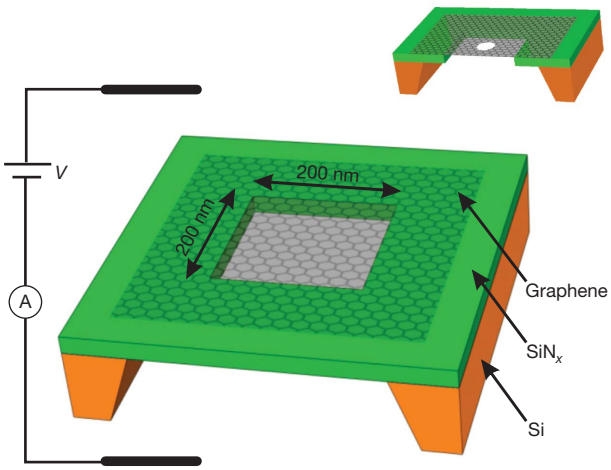

Figure 1 | Diagram of our experiments. A graphene membrane was mounted over a 200×200 nm aperture in SiN_x suspended across a Si frame (not to scale). The membrane separates two ionic solutions (not shown) in contact with Ag/AgCl electrodes (thick lines top and bottom, connected via a voltage source and a sensitive ammeter, A). Inset, cross-section through the Si frame, SiN_x aperture, and the graphene membrane through which a nanopore has been drilled.

[1]Department of Physics, Harvard University, Cambridge, Massachusetts 02138, USA. [2]School of Engineering and Applied Sciences, Harvard University, Cambridge, Massachusetts 02138, USA. [3]Department of Materials Science and Engineering, Massachusetts Institute of Technology, Cambridge, Massachusetts 02139, USA. [4]Department of Electrical Engineering and Computer Science, Massachusetts Institute of Technology, Cambridge, Massachusetts 02139, USA. [5]Department of Molecular and Cellular Biology, Harvard University, Cambridge, Massachusetts 02138, USA.

Table 1 | Trans-membrane conductance of as-grown graphene

Solution	Graphene conductance (pS)	Solution conductivity (10^{-3} S m^{-1})	Cation hydration energy[20] (eV)
CsCl	67 ± 2	1.42	3.1
RbCl	70 ± 3	1.42	3.4
KCl	64 ± 2	1.36	3.7
NaCl	42 ± 2	1.19	4.6
LiCl	27 ± 3	0.95	5.7

The membrane separated two compartments, each containing only the ionic solutions indicated in column 1. Conductances were determined from voltage bias scans between +100 mV and −100 mV. All data shown here are from the same device, the graphene membrane of which was suspended across a 200 × 200 nm SiN_x frame. The absolute magnitudes of the conductances varied by a factor of two from membrane to membrane, but the general trend and order of conductance differences with the five solutions was invariant for all membranes.

mobility of potassium (i = K) and chloride (i = Cl) ions used in our measurements. The linear dependence of conductance on diameter follows from the current density being sharply peaked at the pore's perimeter for an infinitely thin membrane. For membranes thicker than the pore diameter, the conductance becomes proportional to the nanopore area. For finite but small thicknesses, we rely on computer calculations to predict the conductance.

In agreement with equation (1), the trans-electrode conductance of pores with diameters ranging from 5 to 23 nm (Fig. 3) exhibited a near-linear dependence on pore diameter. Figure 3 also shows the results of computer calculations of nanopore ionic conductance in an idealized uncharged, insulating membrane, as a function of pore diameter and membrane thickness. They are obtained by numerically solving the Laplace equation for the ionic current density, with appropriate solution conductivity and boundary conditions, and integrating over the pore area to get the conductance (Methods). The results are equivalent to the solution of the Poisson–Nernst–Planck equation in the same geometry. We refer to the membrane thickness L used in this idealized model as the graphene insulating thickness, or L_{IT}. The best fit to the measured pore conductance data in Fig. 3 yields $L_{IT} = 0.6\,(+0.9, -0.6)$ nm, with the uncertainty determined from a least-squares error analysis. Figure 3 also shows the theoretical results for $L_{IT} = 2.0$ nm and $L_{IT} = 10.0$ nm.

Measurements of nanopore conductance when a long chain polymer of DNA passes through the nanopore provide an alternative method of evaluating L_{IT}. In such experiments, the negatively charged DNA molecules are electrophoretically drawn to and driven through a nanopore. Each insulating molecule passing through the pore transiently reduces, or blocks, the ionic current in a manner that reflects both polymer size and conformation[9]. As shown below, such

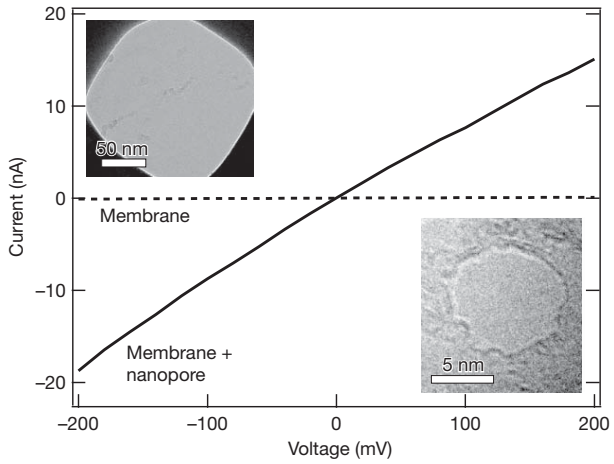

Figure 2 | Trans-electrode *I–V* curves. Results for an as-grown graphene membrane (dashed line) and a membrane with an 8-nm pore (solid line). The ionic conductance of the pore is quantitatively in agreement with the modelling presented in the text. Applying bias voltages in excess of ~250 mV gradually degraded the insulating properties of the membranes. Insets, TEM images: top, a mounted graphene membrane; bottom, the 8-nm pore.

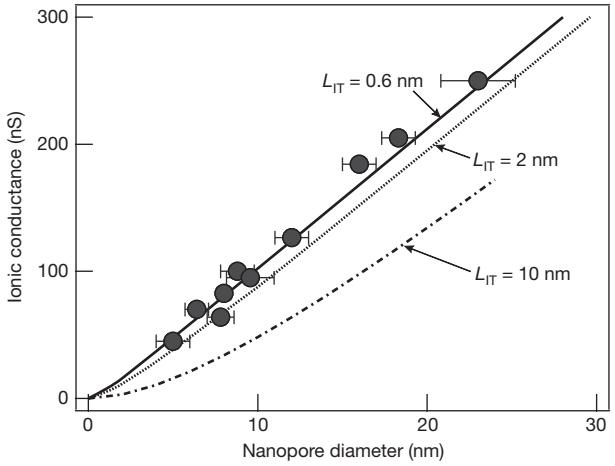

Figure 3 | Graphene nanopore conductance. Filled circles, experimental results with a 1 M KCl solution of conductivity $\sigma = 11$ S m^{-1}. Solid curve, modelled conductance of a 0.6-nm-thick insulating membrane, which is the best fit to the experimentally measured conductances. Error bars, s.d. of four diameter measurements along different nanopore axes. Modelled conductances for a 2-nm-thick membrane (dotted line) and a 10-nm-thick membrane (dashed-dotted line) are presented for comparison.

DNA experiments also reveal the membrane thickness and the nanopore diameter. The results using a 5-nm pore in graphene and double-stranded DNA molecules are shown in Fig. 4. The insets show two single-molecule translocation events. In the event shown in the right inset, a molecule passes through the pore in an unfolded linear fashion. In contrast, the left inset shows an event in which the molecule is folded over on itself when it enters the pore, increasing the current blockade for a short time[9]. Each single-molecule translocation event can be characterized by two parameters: the average current drop, or blockade, and the duration of the blockade, which is the time it takes for the molecule to completely translocate through the pore. The scatter plot in Fig. 4 shows the value of these parameters for each of 400 DNA single-molecule events. The

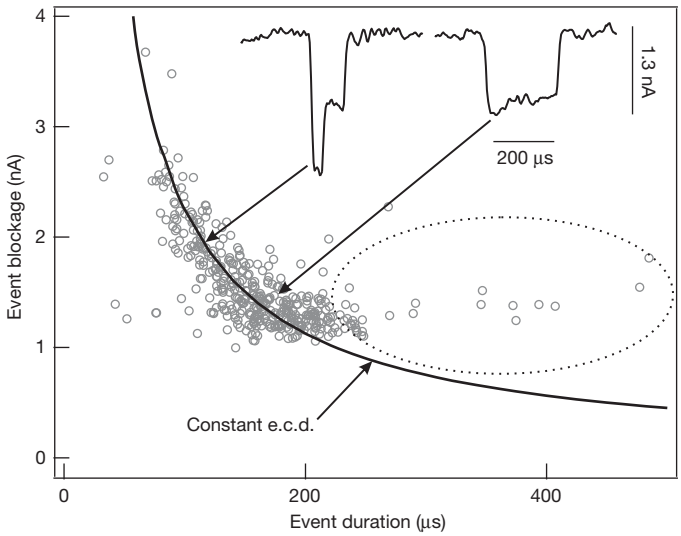

Figure 4 | Average nanopore current blockades versus blockade duration during DNA translocation. DNA (16 μg ml^{-1}) was electrophoretically driven through a 5-nm-diameter graphene pore by an applied voltage bias of 160 mV. The graphene membrane separated two fluid cells containing unbuffered 3 M KCl solutions, pH 10.4. Insets, typical current–time traces for two translocation events sampled from among those pointed to by the arrows. The hyperbolic curve corresponds to freely translocating events at a fixed e.c.d. (electronic charge deficit; ref. 12). Encircled events are delayed by graphene–DNA interactions.

characteristic shape of these data is similar to that obtained in silicon nitride nanopore experiments[9], where almost all the events, folded and unfolded, fall near a line of constant electronic charge deficit (e.c.d.): that is, regardless of how the otherwise identical molecules are folded, each blocks the same amount of ionic charge movement through the pore during the total time it takes each molecule to move through the pore[9]. Such molecules pass through the pore uninhibited by sticking to the graphene surface. The few events that are encircled in the plot do not satisfy this condition, and their long translocation times indicate graphene–DNA interactions, which slow their translocation through the nanopore.

We compare the experimentally determined open pore and DNA blocked pore conductance with numerical solutions (as above, and see Methods), where the membrane thickness and the nanopore diameter are the fitting parameters. Using the observed mean current blockade $\Delta I = 1.24 \pm 0.08$ nA during translocation of unfolded double-stranded DNA of diameter 2.0 nm (ref. 10), and the observed conductance of the pore when DNA is absent ($G = 105 \pm 1$ nS), we calculate that $L_{IT} = 0.6 \pm 0.5$ nm, in excellent agreement with the value deduced above from open pore measurements alone. The pore diameter $d = 4.6 \pm 0.4$ nm deduced from these calculations also agrees with the geometric diameter of 5 ± 0.5 nm obtained from transmission electron microscopy (TEM) of this pore.

The best fit value from both experiments, $L_{IT} = 0.6$ nm, agrees with molecular dynamics simulations showing the graphene–water distance to be 0.31–0.34 nm on each side of the membrane[11,12]. L_{IT} might also be influenced by the typical presence of immobilized water molecules and adsorbed ions in the Stern layer[13]. On the other hand, theoretical studies argue against any immobilized water layer on graphene, and experimental measurements support an anomalously high slip between water and an internal curved carbon nanotube surface[11,14]. Although very little is actually known about the surface chemistry of specifically adsorbed ions on single-atom-thick graphene layers[1], measurements of the ionic current through the inner volume of carbon nanotubes with diameters less than 1 nm (ref. 15) may indicate that ions are not immobilized on these graphitic surfaces at all. Our subnanometre values for L_{IT} support this view.

The extremely small L_{IT} value we obtain suggests that nanopores in graphene membranes are uniquely optimal for discerning spatial or chemical molecular structure along the length of a molecule as it passes through the pore. Although polymer translocation speeds and electronics bandwidth currently preclude a direct measurement of a nanopore's spatial or geometric resolution limit[16], we can gain insight into the system's limit by numerically modelling the resolution obtainable as a function of L_{IT}.

The model uses a long, insulating, 2.2-nm-diameter cylinder symmetrically translocating through the centre of a 2.4-nm diameter nanopore. At one position along its length, the cylinder diameter changes discontinuously from 2.2 nm to 2.0 nm. Solving for the ionic conductance for this geometry as the discontinuity passes through the pore, we obtain the predictions shown in Fig. 5. The decreasing blockade (increasing conductance) of a pore is clearly seen as the large-diameter portion of the cylinder leaves the pore. The results of calculations for two L_{IT} values are shown. For the conservative $L_{IT} = 1.5$ nm, the spatial resolution (defined as the distance over which the conductance changes from 75% of its greatest value to 25% of that value) is given by $\delta z = 7.5$ Å, whereas the best-fit value $L_{IT} = 0.6$ nm leads to $\delta z = 3.5$ Å. We conclude from our experiments and modelling that a pore in graphene is inherently capable of probing molecules with subnanometre resolution. Functionalizing the graphene nanopore boundary[5] or observing its local in-plane electrical conductance during translocations may provide additional or alternative means of further increasing the resolution of this system.

We have demonstrated that an atomically thin sheet of graphene can be fabricated into a new structure—a trans-electrode membrane—that attracts cations and anions to its opposing surfaces with subnanometre proximity. Interactions between anions and cations

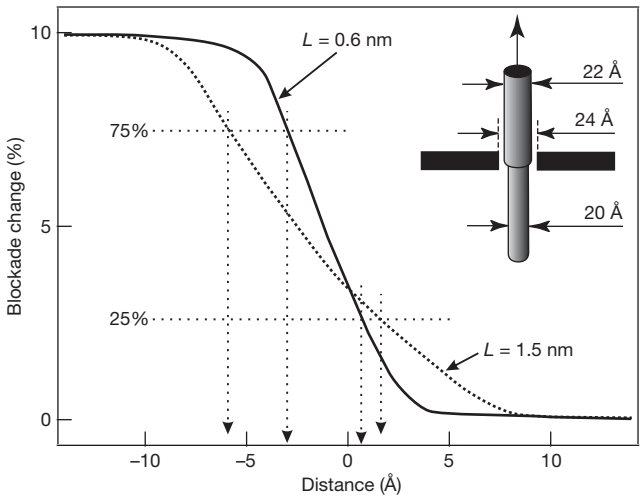

Figure 5 | Geometric resolution. Modelled nanopore conductance as the abrupt diameter decrease of a model molecule (inset) translocates through a 2.4-nm pore. The attainable resolution for two membranes of different insulating thicknesses (0.6 nm, solid curve; 1.5 nm, dotted curve) is assumed to be achieved when the measured current through the nanopore changes from 75% to 25% of the maximum blockade change that would occur as the model molecule translocates through the nanopore.

across the interface are mediated by the graphene and the high electric fields this interface supports. Owing to its extreme thinness, the graphene layer's in-plane electronic conductance is also sensitive and available for probing the interfacial environment. With electrical contacts applied to the graphene electrode, this conductance can be measured even for very small area ($<1 \times 1$ μm) membranes, making the trans-electrode a particularly interesting device for chemical sensing and surface electrochemistry studies. Surface chemical reactions can be probed at very few charged sites by ionic current measurements through a nanopore[17]. In-plane electronic and nanopore ionic current measurements with trans-electrode devices would greatly extend this methodology. Many opportunities exist for modifying the properties of the trans-electrode device and its sensitivity (for example, by changing membrane thickness, doping and defects). The interactions at, and between, the two liquid–solid interfaces in graphene may well hold many surprises and applications.

After this Letter was submitted, the concept of using graphene nanopores to characterize DNA polymers appeared online[18,19]. We believe that the present Letter provides the first realization of DNA translocation through atomically thin graphene.

METHODS SUMMARY

Graphene grown via CVD on the surface of a nickel substrate[2] was spin-coated with an adhesion film of MMA/MAA (methyl-methacrylate/methacrylic acid) copolymer adhesion film. The nickel was etched away overnight in a 1 M HCl solution. The film was placed graphene side down across a 200-nm square aperture in the SiN_x coating on a windowed Si chip (Fig. 1). The adhesion film was dissolved and washed away with acetone. Nanometre-scale pores in the graphene were electron-beam-drilled in a 200-keV JEOL 2010 transmission electron microscope[7]. The fluidic cell was fashioned from polyether-ketone with PDMS fluidic seals on each side of the chip. Ionic current measurements through the as-produced graphene membranes or graphene membranes with nanopores were performed by standard electrophysiology methods[20,21].

Full Methods and any associated references are available in the online version of the paper at www.nature.com/nature.

Received 12 April; accepted 27 July 2010.
Published online 18 August 2010.

1. Geim, A. K. Graphene: status and prospects. *Science* **324,** 1530–1534 (2009).
2. Reina, A. *et al.* Large area, few-layer graphene films on arbitrary substrates by chemical vapor deposition. *Nano Lett.* **9,** 30–35 (2009).

3. Reina, A. *et al.* Growth of large-area single- and bi-layer graphene by controlled carbon precipitation on polycrystalline Ni surfaces. *Nano Res.* **2,** 509–516 (2009).
4. Ferrari, A. C. *et al.* Raman spectrum of graphene and graphene layers. *Phys. Rev. Lett.* **97,** 187401 (2006).
5. Sint, K., Wang, B. & Kral, P. Selective ion passage through functionalized graphene nanopores. *J. Am. Chem. Soc.* **130,** 16448–16449 (2008).
6. Zwolak, M., Lagerqvist, J. & Di Ventra, M. Quantized ionic conductance in nanopores. *Phys. Rev. Lett.* **103,** 128102 (2009).
7. Storm, A. J., Chen, J. H., Ling, X. S., Zandbergen, H. W. & Dekker, C. Fabrication of solid-state nanopores with single-nanometre precision. *Nature Mater.* **2,** 537–540 (2003).
8. Hall, J. E. Access resistance of a small circular pore. *J. Gen. Physiol.* **66,** 531–532 (1975).
9. Li, J., Gershow, M., Stein, D., Brandin, E. & Golovchenko, J. DNA molecules and configurations in a solid-state nanopore microscope. *Nature Mater.* **2,** 611–615 (2003).
10. Zwolak, M. & DiVentra, M. Physical approaches to DNA sequencing and detection. *Rev. Mod. Phys.* **80,** 141–165 (2008).
11. Alexiadis, A. & Kassinos, S. Molecular simulation of water in carbon nanotubes. *Chem. Rev.* **108,** 5014–5034 (2008).
12. Werder, T., Walther, J. H., Jaffe, R. L., Halicioglu, T. & Koumoutsakos, P. On the water-carbon interaction for use in molecular dynamics simulations of graphite and carbon nanotubes. *J. Phys. Chem. B* **107,** 1345–1352 (2003).
13. Bard, A. J. & Faulkner, L. R. *Electrochemical Methods. Fundamentals and Applications* 2nd edn, Ch. 13, 534–579 (Wiley & Sons, 2001).
14. Holt, J. K. *et al.* Fast mass transport through sub-2-nanometer carbon nanotubes. *Science* **312,** 1034–1037 (2006).
15. Liu, H. *et al.* Translocation of single-stranded DNA through single-walled carbon nanotubes. *Science* **327,** 64–67 (2010).
16. Branton, D. *et al.* The potential and challenges of nanopore sequencing. *Nature Biotechnol.* **26,** 1146–1153 (2008).
17. Hoogerheide, D. P., Garaj, S. & Golovchenko, J. A. Probing surface charge fluctuations with solid-state nanopores. *Phys. Rev. Lett.* **102,** 256804 (2009).
18. Schneider, G. F. *et al.* DNA translocation through graphene nanopores. *Nano Lett.* doi:10.1021/nl102069z (published online 7 July 2010).
19. Merchant, C. A. *et al.* DNA translocation through graphene nanopores. *Nano Lett.* doi:10.1021/nl101046t (published online 23 July 2010).
20. Hille, B. *Ion Channels of Excitable Membranes* 3rd edn, Ch. 1 1–22 (Sinauer Associates, 2001).
21. Kasianowicz, J. J., Brandin, E., Branton, D. & Deamer, D. W. Characterization of individual polynucleotide molecules using a membrane channel. *Proc. Natl Acad. Sci. USA* **93,** 13770–13773 (1996).

Acknowledgements This work was funded by a grant (number R01 HG003703) to J.A.G. and D.B. from the National Human Genome Research Institute, National Institutes of Health.

Author Contributions Graphene samples were grown by J.K. and A.R. Experiments and calculations were performed by S.G. Other activities, including data interpretation, conclusions and manuscript writing, were performed collaboratively at Harvard University by S.G., W.H., D.B. and J.A.G.

Author Information Reprints and permissions information is available at www.nature.com/reprints. The authors declare no competing financial interests. Readers are welcome to comment on the online version of this article at www.nature.com/nature. Correspondence and requests for materials should be addressed to J.A.G. (golovchenko@physics.harvard.edu) or S.G. (sgaraj@fas.harvard.edu).

METHODS

Graphene preparation. Continuous large-scale graphene films were synthesized by CVD on 500-nm-thick nickel film evaporated on top of a Si/SiO_2 wafer, using a recently published method[2]. Raman spectroscopy, TEM and selected area diffraction studies[2,3] show the graphene film to be of excellent quality and mostly (87%) a mixture of one- and two-layer-thick domains, with domain sizes of $\sim$10 μm. Thicker regions of three or more graphene layers, easily distinguished by colour contrast in an optical microscope, cover only a small fraction of the total surface. If thicker regions or domain boundaries were found within the 200×200 nm active region of a device, that device was discarded.

Graphene was transferred to a carrier Si/SiN_x chip using a transfer technique similar to one previously published[2]. First, the Si/SiO_2/Ni wafer with synthesized graphene was coated with MMA-MAA copolymer (MMA(8.5)MAA EL9, Microchem Corp.) and cut into 0.5 mm $\times$ 0.5 mm pieces. These pieces were immersed for $\sim$8 h in 1 M HCl solution to etch away the Ni film and free the graphene/polymer membrane, which was transferred to distilled water on which the graphene/polymer floated, graphene-side down. A carrier Si chip coated with $\sim$250-nm-thick SiN_x was used to scoop up the floating graphene/polymer film, taking care that the graphene/polymer film was stretched over the central region of the chip. The central region of the chip had been microfabricated using standard anisotropic etch techniques to leave a $\sim 50 \times 50$ μm area of the SiN_x coating as a free-standing SiN_x membrane into which a square window, $\sim 200 \times 200$ nm, had been drilled using a focused ion beam. Nitrogen gas flow was used to firmly press the graphene against the chip's surface. This led to expulsion of a small amount of liquid from under the graphene, which adhered strongly and irreversibly to the carrier chip's SiN_x coating. The polymer on top of the graphene was removed under a slow drip of acetone, followed by subsequent immersions in acetone, dichloroethane and finally isopropanol.

To remove any residues from the graphene film, the chip was subsequently immersed in 33 wt% solution of KOH at room temperature for 1 min, then vigorously rinsed with isopropanol and ethanol. To avoid damage to the suspended free-standing portion of the graphene film, the chip was critical-point dried. Finally, the chip was loaded into a rapid thermal annealer and heated to 450 °C in a stream of gas containing 4% H_2 in He for 20 min to drive off any remaining hydrocarbons. To avoid recontamination, the chip was immediately loaded into a transmission electron microscope for further processing.

A single nanometre-sized pore was drilled through the graphene membrane using a focused electron beam in a JEOL 2010 FEG transmission electron microscope operated at 200 kV acceleration voltage. Methods to form more reproducibly dimensioned nanopores in graphene are being developed, but we determined the nanopore size by electron microscope visualization in a well spread electron beam so as to keep the total electron exposure of the graphene membrane to a minimum. The reported nanopore diameter is an average of four measurements along different nanopore axes, as determined from calibrated transmission electron micrographs using DigitalMicrograph software (Gatan). The error bar represents the standard deviation of those measurements, and reflects irregularities and deviations of the pore perimeter from perfect circularity. If the chip or TEM holder had any contaminating organic residue, amorphous carbon was seen to visibly deposit under the electron beam. Such devices were discarded. After drilling the nanopore, the graphene nanopore chips that were not immediately investigated were kept under a clean vacuum of $\sim 10^{-5}$ torr.

Fluidic cell preparation. The chip-mounted graphene was inserted between the two half-cells of a custom-built microfluidic cassette made of polyether-etherketone. The two sides of the chip were sealed with PDMS gaskets. The opening of the gasket that pressed against the graphene film on the Si/SiN_x carrier chip (Fig. 1) had an inside diameter of $\sim$100 μm. Consequently, the gasket orifice was smaller than the dimensions of the graphene film (0.5 $\times$ 0.5 mm), and completely sealed off the graphene edge from the electrolyte. On the opposite side of the chip, the electrolyte is in contact with the graphene membrane only through the 200-nm-wide square window in the SiN_x membrane. Note that there is a large area difference between the two graphene faces in contact with the electrolyte (a circular area of 100 μm diameter versus a square 200×200 nm area). This difference in contact area may in part explain the small conductance asymmetries and nonlinearities in our graphene *I–V* curves.

The two half-cells were first filled with ethanol to facilitate wetting of the chip surface. The cell was then flushed with deionized water, followed by 1 M KCl solution with no buffer. To avoid any potential interaction between the graphene and the solutes which could affect the measurements of graphene thickness and DNA translocations, all the electrolytes were kept as simple as possible and were unbuffered. With the exception of solutions used in the experiment of Fig. 4, all solution pHs ranged over only 0.2 pH units, from 5.09 to 5.29, as measured both before and after use in the described experiments. The pH of the solution used for the Fig. 4 experiment was adjusted to pH 10.4 with KOH just before use. Because the design of our microfluidic cassette maintained the solution largely out of contact with ambient atmosphere, the pH varied less than 0.2 pH units during the course of the Fig. 4 experiments.

Measurements. Ag/AgCl electrodes in each half-cell were used to apply an electric potential across the graphene membranes and to measure ionic currents[20,21]. The current traces were acquired using an Axopatch 200B (Axon Instruments) amplifier, which was connected to an external eight-pole Bessel low-pass filter (type 90IP-L8L, Frequency Devices) operating at 50 kHz. The analogue signal was digitized using a NI PCI-6259 DAQ card (National Instruments) operating at 250-kHz sampling rate and 16-bit resolution. The experiment was controlled through IGOR Pro software.

For DNA translocation measurements, the microfluidic cell was flushed with 3 M KCl solution at pH 10.4, containing 1 mM EDTA. High KCl concentration and high pH were found to minimize DNA–graphene interaction. We introduced 10-kilobase-pair restriction fragments of double-stranded λ-phage DNA molecules to the *cis* chamber. The DNA translocation events were analysed with MATLAB using a fitting function that consisted of multiple square pulses convoluted with an appropriate Bessel filter function to mimic the recording conditions.

Conductivities of all the solutions mentioned in the main text were measured using an Accumet Research AR50 conductivity meter, which had been calibrated using conductivity standard solutions (Alfa Aesar, product numbers 43405, 42695, 42679). All the fluidic experiments were performed under temperature-controlled laboratory conditions, at 24 °C.

To investigate the contribution from electrochemical (Faradic) currents, a large-area graphene film ($\sim 2 \times 4\ mm^2$) was transferred to a glass slide and contacted at one end with silver paint attached to a metallic clip over which wax insulation was placed. The exposed end of the film was immersed in 1 M KCl electrolyte with a Ag/AgCl counter electrode, and the electrochemical *I–V* curves were measured in the same voltage range as used in the trans-electrode experiments. After normalizing for the surface area, we conclude that any electrochemical currents in the trans-electrode devices were three orders of magnitude too small to account for the approximately picoamp currents measured through the as-grown graphene membranes in Table 1.

Simulations. The numerical simulations were performed using the COMSOL Multiphysics finite element solver in appropriate three-dimensional geometry with cylindrical symmetry along the axis of the nanopore. We solved the full set of Poisson–Nerst–Planck equations in the steady-state regime. In the range of physical parameters of interest (high KCl concentration and small applied voltage), the numerical simulation solution was found not to differ significantly from the solution of the Laplace equation with fixed conductance, which has significantly less computational penalty. A DNA molecule was modelled as a long stiff insulating rod of diameter 2 nm which threads through the centre of the nanopore. For lateral resolution calculations, we added a step of 2.2-nm diameter to the DNA model, and we calculated the change in the ionic current as the discontinuity is translocated through the centre of the pore. The total ionic current was calculated by integrating current density across the diameter of the nanopore.